WAKE FIELD SIMULATIONS FOR THE VACUUM CHAMBER TRANSITIONS OF THE ILC DAMPING RING.*

M. Korostelev†, A. Wolski, University of Liverpool and the Cockcroft Institute, UK.
N. Collomb, J. Lucas, STFC Technology, Daresbury Laboratory, UK.
O. B. Malyshev, STFC ASTeC, Daresbury Laboratory, UK

Abstract

Vacuum chamber transitions of the ILC damping rings mainly associated with BPM insertions may make a significant contribution to the overall machine impedance. Since most transitions are not azimuthally symmetric, commercial 3D codes based on the finite integration method have been used to compute their wake fields. The results for selected vacuum chamber components are presented in this paper, together with some estimates of the impact of the wake fields on the beam dynamics in the damping rings.

INTRODUCTION

The damping rings of the International Linear Collider (ILC) have strict specifications for beam quality and stability. The present baseline of the ILC damping rings [1] is a 5 GeV "racetrack" design (two arcs connected by straights) of roughly 6 km circumference. As a main part of the beam diagnostics system, high resolution beam position monitors (BPM) are expected to be installed downstream of each quadrupole. There may be as many as 690 BPMs in total.

The technical design of the BPM insertion together with other vacuum system components for the ILC damping ring have been developed by STFC/ASTeC and the Cockcroft Institute. Design work for the BPMs is focused on meeting the performance specifications while keeping as low as possible the contribution to the machine impedance and impact on the beam dynamics.

In this paper we consider two BPM designs, referred as the "original" and "new" BPM models of the ILC damping ring. The detailed description of the original BPM model can be found in Ref. [2]. Our preliminary calculations of impedance for the original BPM model [2] did not give reliable results above 3 GHz, because of limitations inherent in the techniques that were used. To improve the accuracy and reliability of the wake field calculations, we decided to employ time-domain simulations. The wake field studies presented in this paper were carried out using a three-dimensional electromagnetic code, CST Particle Studio [3] for both the original and the new models.

In the CST time-domain simulations, Perfect Boundary Approximation (PBA) is implemented for the discretization of geometrical objects where the structure is represented by a hexagonal mesh. The accuracy of the e.m. field solution is determined by the mesh resolution, and the (optional) use of adaptive mesh refinement features.

* Work supported by the Science and Technology Facilities Council.
† maxim.korostelev@stfc.ac.uk

NEW BPM DESIGN

An alternative new bellows design with improved rf shielding, based on a design from INFN-LNF [4], has been implemented in the new BPM model as illustrated in Fig. 1. The features of the new design are the following:

- The new bellows design uses a single multi-strip shield, unlike the original design that used a two piece inner/outer shield. This new arrangement eliminates the alignment issues that were possible with the original design.
- The new design allows a degree of radial adjustment with the shield strips, providing a more reliable and effective fit.
- Visual assembly of internal components (i.e. fitting the shield over the inner shield sleeve) is greatly improved.

The buttons assembly in the new design is identical to that in the original BPM design. Note that the buttons themselves are not shown in Fig. 1. Each BPM is mounted on an individual stand, to provide mechanically isolation from the vacuum chamber. We expect that a narrow gap of 1 mm between the rf shielding strips should provide sufficient vacuum transparency.

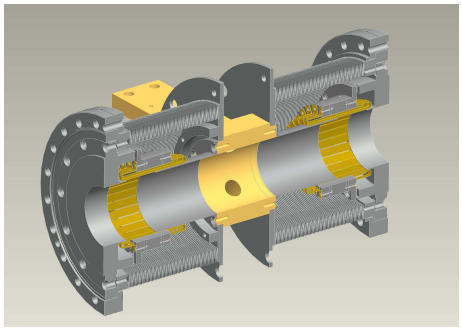

Figure 1: New BPM model.

WAKE FIELD ANALYSIS

The complicated structure of our BPM models, including many complex details with different sizes and radius of curvature, has to be approximated by a large number of mesh cells to achieve good accuracy for the e.m. field solution. On the other hand, a high mesh density dramatically

increases the required CPU time and memory usage. Moreover, numerical errors tend to accumulate.

The total length of the original structure is 36 cm while the new structure is 40 cm long. The effective volumes 3990 cm^3 and 4070 cm^3 of the original and new BPM structure respectively are mapped by 150 million mesh cells, corresponding to 26 lines per wavelength with a constraint on the maximum mesh step width < 0.17 mm in the longitudinal direction. The peak memory usage for computing 150 million mesh cells in our case is around 32 GB. The density of the generated hexagonal mesh is not uniform: the step varies from 0.05 mm to 0.8 mm, and generally depends on the complexity of the surface.

Open boundary condition are assigned to the end cross sections of both models. At the output of each BPM pickup is a 50 Ω coaxial line connector, terminated at a wave port. Because of the transverse four-fold symmetry of the models, it is necessary to simulate only a quarter of each structure for the case of a bunch traversing the structure on-axis.

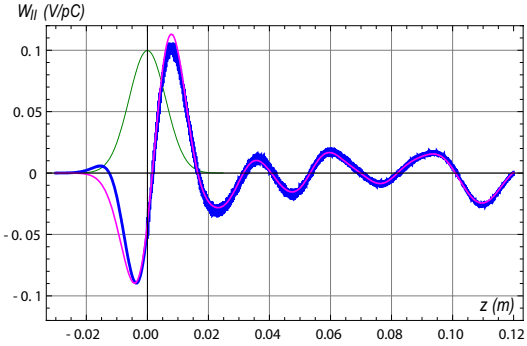

Figure 2: Wake potential for original BPM model (blue) and wake potential restored from the wake function (magenta).

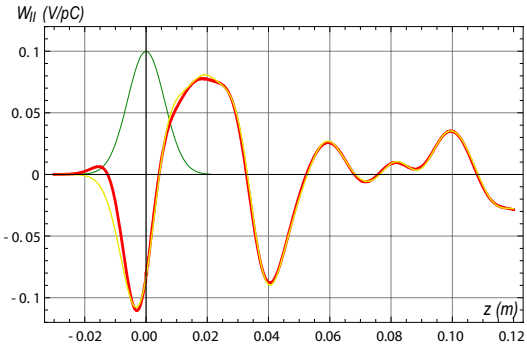

Figure 3: Wake potential of the new BPM model (red) and wake potential restored from the wake function (yellow).

Fig. 2 and Fig. 3 show the longitudinal wake potentials excited by a Gaussian relativistic electron bunch in the original and new BPM structures, respectively. The electron bunch has a charge of 3.2 nC (bunch population 2×10^{10}) and rms length of 6 mm in each case. The normalized charge density of the given bunch is indicated by the green curve in each figure.

Small oscillations (numerical noise) around the wake potential in Fig. 2 are caused by the accumulation of numerical errors during computation, because of the high density of the mesh. Moreover, a small unphysical wake occurs ahead of the bunch. We expect that this artefact may be reduced if a smaller longitudinal mesh step can be applied.

The wake potential calculated for the original BPM model shows that the inductive part of the impedance dominates at low frequencies: the shape of the wake potential is approximately proportional to the gradient of the charge density. Usually, an inductive wake field is caused by objects with discontinuities that are small compared to the bunch length. Inductive structures tend to lead to bunch lengthening.

The wake potential for the new model, shown in Fig. 3, exhibits both inductive and resistive characteristics of the structure impedance: in terms of an RLC circuit the wake potential can be approximated, as $LdI(t)/dt - RI(t)$, where the resistive term has little impact on bunch lengthening, compared to a pure inductive structure. Broad-band rf cavities can demonstrate similar characteristic behavior for the wake potential, for certain bunch lengths. As can be seen from Fig. 1, strips of the rf shielding connected to their supports form an rf cavity-like structure that leads to inductive and resistive wakes. In addition, the structure begins to reveal (albeit weakly) capacitive properties associated with HOMs.

Wake field analysis carried out for the BPM buttons only, shows that a TE mode of around 7.5 GHz is trapped in the gap of 0.9 mm between the button and its housing. Detailed studies of this issue will be carried out in the future using a frequency-domain eigenmode solver, usually applied to narrow-band resonant structures.

The loss factor at a bunch length of 6 mm is 0.044 V/pC for the new BPM model, and 0.01 V/pC for the original BPM model. The loss factor for the original BPM model is smaller by a factor of 4.4, because of its weak resistive properties. The loss factor produced by the BPM buttons themselves is 0.007 V/pC. The average dissipated power per BPM insertion is 12.3 W for the original model and 54.4 W for the new model.

The wake potentials have been computed and integrated over a distance of 1 m to provide sufficient resolution for the calculation of the impedance. The impedance $Z_{\parallel}(\omega)$ may be found from:

$$-cZ_{\parallel}(\omega) = \frac{\int_{-\infty}^{\infty} W_{\parallel}(z)e^{-i\frac{\omega z}{c}}dz}{\int_{-\infty}^{\infty} \lambda(z)e^{-i\frac{\omega z}{c}}dz}. \qquad (1)$$

Applying an inverse Fourier transform to the impedance with the limits ±25 GHz, the wake functions (Green's functions) shown in Fig. 4 have been obtained for each BPM model. An impedance above these limits cannot be considered in our case, because 99.8% of the charge in a 6 mm Gaussian bunch is contained within the frequency range of ±25 GHz.

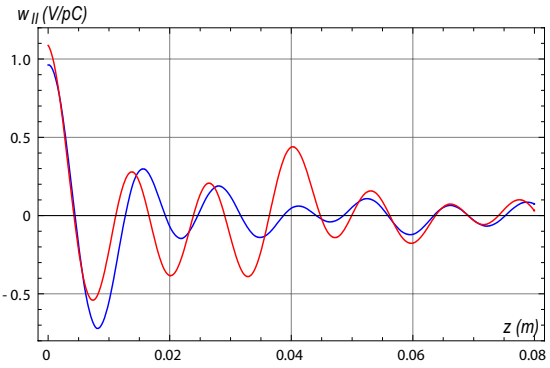

Figure 4: Wake functions of original (blue curve) and new (red curve) BPM models.

Comparisons of the wake potentials computed by CST, and the wake potentials evaluated as a convolution of the charge distribution and the wake functions (in Fig. 4) are shown in Fig. 2 and Fig. 3. Generally, they are in good agreement, apart from the region ahead of the bunch distribution. The discrepancy in this region may be a result of the upper limit imposed on the inverse Fourier transform of the impedance, which limits the accuracy of the wake function in the vicinity of $z = +0$. Another possible reason for the discrepancy is the existence of the small unphysical wake mentioned above. A wake field analysis for a shorter bunch length is needed, in order to get a more accurate description of the wake function close to $z = +0$. However, this will require an increase in computational effort, since the mesh refinement in CST PS depends on the bunch length.

BUNCH LENGTHENING

The change in the longitudinal distribution of particles in a bunch in the presence of a wake field (potential well distortion) can be found from the Haissinski equation [5]:

$$\lambda(z) = K \exp\left\{ -\frac{z^2}{2\sigma_z^2} - \frac{4\pi\varepsilon_0 r_e N_b}{\alpha_p \gamma C \sigma_\delta^2} \int_0^z W_\parallel(z')dz' \right\}. \quad (2)$$

Here, $\lambda(z)$ is the charge distribution, normalised so that $\int_{-\infty}^{\infty} \lambda(z)dz = 1$; $W_\parallel(z') = \int_{z'}^{\infty} \lambda(z'')w_\parallel(z'-z'')dz''$; $w_\parallel$ is the wake function; C is the ring circumference; N_b is the bunch population; and $\varepsilon_0 = 8.85 \times 10^{-12}$ F/m is the vacuum permittivity.

Beyond some threshold value for the total number of particles in the bunch, the bunch distribution becomes unstable. Solutions to the Haissinski equation exist only below the instability threshold. For some particular cases below threshold (e.g. for purely inductive, resistive, or capacitive wakes) analytical solutions can be found; but in general, numerical solutions are required.

To estimate bunch lengthening for the wake functions obtained above, we have solved Eq. 2 using a numerical, iterative technique. For a total of 690 BPMs, the rms bunch length as a function of bunch population N_b is shown in Fig. 5. It can be seen that the inductive wake field induced by the original BPM model has a slightly larger impact on the bunch lengthening than the inductive-resistive wake of the new BPM.

For a bunch population $N_b = 2 \times 10^{10}$, the longitudinal charge densities in the presence of the original and new BPM wake fields are shown in Fig. 5. A Gaussian bunch of rms length 6 mm (black curve in Fig. 5) deforms to shapes with rms length of 6.15 mm with the new BPMs, and 6.21 mm with the original BPMs.

We find that beyond a bunch population of 2.2×10^{10} our numerical iteration procedure for solving the Haissinski equation fails to converge properly if the correct normalisation of the charge distribution is imposed. This may indicate an instability (turbulent bunch lengthening) threshold beyond $N_b = 2.2 \times 10^{10}$. By relaxing the normalisation condition, however, it is still possible to make an estimate of the rms bunch length above this bunch population.

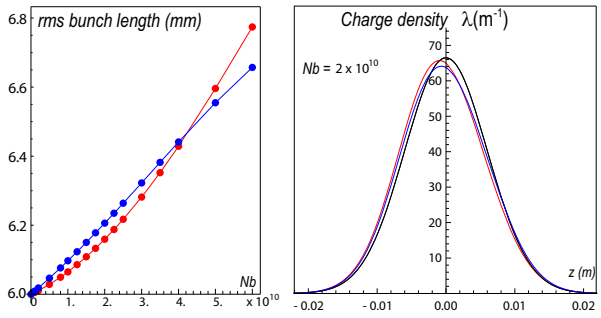

Figure 5: RMS bunch length as a function of bunch population (left plot) and longitudinal bunch shapes in the presence of the original (blue) and new (red) BPM wake fields (right plot).

CONCLUSIONS

The new BPM model has some benefits in mechanical design, specifically addressing possible alignment issues during assembly. A comparison of the wake fields for the original and new BPM models shows a marginal reduction in bunch lengthening, but also some increase in power load. There is a possible instability threshold just above the nominal bunch population of 2×10^{10} particles: this needs more careful study.

REFERENCES

[1] https://wiki.lepp.cornell.edu/ilc/pub/Public/DampingRings/WebHome/

[2] M. Korostelev, A. Wolski et al, "Beam coupling impedance in the ILC damping rings," proceedings of EPAC'08, Genoa, Italy (2008).

[3] Computer Simulation Technology, http://www.cst.com/

[4] F. Marcellini, G. Sensolini, private communication.

[5] J. Haissinski, Nuovo Cimento 18B, 72 (1973).